ACS APPLIED MATERIALS & INTERFACES

RESEARCH ARTICLE

www.acsami.org

In Vitro Physicochemical Properties, Osteogenic Activity, and Immunocompatibility of Calcium Silicate−Gelatin Bone Grafts for Load-Bearing Applications

Shinn-Jyh Ding,*[,†,‡] Ming-You Shie,[§] and Chung-Kai Wei[†]

[†]Institute of Oral Biology and Biomaterials Science, Chung Shan Medical University, Taichung City 402, Taiwan

[‡]Department of Dentistry, Chung Shan Medical University Hospital, Taichung City 402, Taiwan

[§]Institute of Biomedical Engineering, National Cheng Kung University, Tainan City 701, Taiwan

ABSTRACT: The use of a composite made of natural polymer gelatin and bioactive calcium silicate resembling the morphology and properties of natural bone may provide a solution to the problem of ceramic brittleness for load-bearing applications. The in vitro bioactivity, degradability, osteogenic activity, and immunocompatibility of three types of calcium silicate−gelatin composite bone grafts were characterized. The osteogenic activity and immunocompatibility were evaluated by incubating the bone grafts with human dental pulp cells. After soaking in a simulated body fluid (SBF) for 1 day, all materials were covered with clusters of "bone-like" apatite spherulites. The control material without gelatin exhibited an insignificant change in strength, degradability, and porosity and a small weight loss of 6% after 180 days of soaking in the SBF solution. In contrast, the soaking time imposed in this study did have a statistically significant effect on compressive strength, porosity, and weight loss of the gelatin-containing composites. After 180 days of soaking, the composite with 10 wt % gelatin lost 47% and 10% in compressive strength and weight, respectively, with a porosity of 23%. However, the presence of gelatin promoted greater cell attachment and proliferation on the composite bone grafts. Pulp cells on the calcium silicate−gelatin bone grafts expressed higher levels of osteocalcin, osteopontin, and bone sialoprotein. The inhibition of inducible nitric oxide synthase and interleukin-1 expression and the activation of interleukin-10 were increased with increasing gelatin content. Overall, these findings provide evidence that composite bone grafts containing 10 wt % gelatin with a high initial strength were bioactive, nontoxic, and osteogenic and may be able to promote bone healing for load-bearing applications.

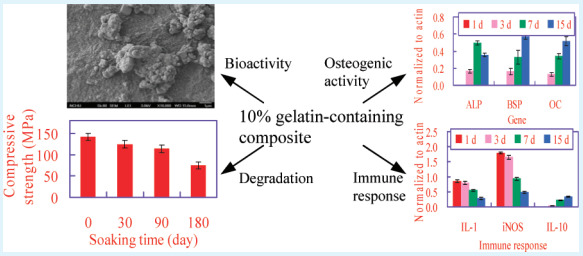

KEYWORDS: calcium silicate, gelatin, bone grafts, bioactivity, osteogenic activity, load-bearing

1. INTRODUCTION

Autografts have been considered the current gold standard because they possess all the characteristics indispensable for new bone growth, namely, osteogenesis, osteoconductivity, and osteoinductivity.[1] However, procurement morbidity and constraints on available quantities hinder autografts as an option for bone repair. A wealth of artificial materials has been proposed as bone graft substitutes. Ideally, synthetic bone graft substitutes should mimic bone morphology and function in order to optimize integration into the surrounding tissue. Bone implants should have a similar strength to that of the cortical/cancellous bone being replaced. The mismatch of mechanical properties between bone implants and natural bone tissues can cause stress shielding and lead to bone resorption.[2] Thus, the development of artificial materials that have ultimately "bone-like" mechanical, physical, and biological properties is desirable. An improved bone graft system for load-bearing applications is desired as there is a constant need.

Silica-based bone grafts, including bioactive glass and calcium silicate ceramic, have attracted significant interest because silica may be associated with the initiation of the mineralization of preosseous tissues.[3] However, the inherent brittleness of ceramics impedes the adaptation of their mechanical properties to those of cortical bone.[4] One strategy to combat this issue could be the use of a polymer to modify ceramic-based bone grafts.[5,6] In one previous study,[7] bioinspired calcium silicate−gelatin composites with high initial strength were successfully developed for load-bearing applications via a simple pressing-hydrothermal method. The 10 wt % gelatin-containing calcium silicate exhibited a compressive strength value of 142 MPa, which is sufficient for its use in load-bearing sites of bone tissue. Additionally, the presence of gelatin provided a favorable environment for MG63 cells, resulting in a larger degree of cell proliferation, differentiation, and formation of mineralized tissue compared to the control material without gelatin. Further investigation of osteogenic activity is necessary because the responses of various cell types to implanted materials are different in various cell culture environments. Human dental pulp cells have the ability to differentiate along the osteoblast lineage and to contribute to the dentinal regeneration process.[8,9] From the viewpoint of clinical applications, they are more suitable than MG63 cells for evaluating the bone tissue response to materials.

Received: August 1, 2011
Accepted: September 27, 2011
Published: September 27, 2011

Furthermore, synthetic bone grafts are foreign to the host, and thus, it is not surprising that the immune response is an important determinant of biocompatibility. The nonspecific (innate) immune system is responsible for initiating rapid and general responses against invasions by foreign objects. It is essential to elucidate the immune response of pulp cells to calcium silicate−gelatin composites for the safe development of such materials.

A prerequisite for the bonding of biomaterials to living bone in vivo is the formation of a "bone-like" apatite layer on the surface of the biomaterial, which is an indicator of bioactivity (the ability to form a chemical bond with living tissue). It is important to evaluate the effects of gelatin on the in vitro physicochemical properties of the bone grafts. As a follow up of the previous study,[7] the purpose of this study was to examine the in vitro activity and degradability of calcium silicate−gelatin composites in a simulated body fluid (SBF) solution and responses of human dental pulp cells to the composites.

2. EXPERIMENTAL SECTION

2.1. Preparation of Specimens. The sol−gel method for the preparation of calcium silicate powder has been described elsewhere.[6,10] Reagent-grade tetraethyl orthosilicate ($Si(OC_2H_5)_4$, TEOS) (Sigma-Aldrich, St. Louis, MO) and calcium nitrate ($Ca(NO_3)_2\cdot 4H_2O$) (Showa, Tokyo, Japan) were used as precursors for SiO_2 and CaO, respectively. Nitric acid was used as the catalyst, and ethanol was used as the solvent. The general sol−gel procedure, including hydrolysis and aging, was used here. Briefly, TEOS was hydrolyzed by the sequential addition of 2 M HNO_3 and absolute ethanol, with 1 h of stirring after each addition. $Ca(NO_3)_2\cdot 4H_2O$ was added to the TEOS solution in an equimolar ratio, and the mixture was stirred for an additional 1 h. The molar ratio of (HNO_3 + H_2O)−TEOS−ethanol was 10:1:10. The solution was sealed and aged at 60 °C for 1 day. After vaporization of the solvent in an oven at 120 °C, the dried gel was heated in air to 800 °C at a heating rate of 10 °C/min for 2 h using a high-temperature furnace and then cooled to room temperature in the furnace to produce a powder. The sintered powders were then ball-milled for 12 h in ethyl alcohol using a Retsch S 100 centrifugal ball mill (Hann, Germany) and dried in an oven at 60 °C. Type B gelatin (isoelectric point at pH = 4.7−5.2) from bovine skin (Sigma-Aldrich) was weighed and dissolved in distilled water at 60 °C until a homogeneous gelatin solution was obtained. To fabricate the organic−inorganic composite, the calcium silicate powder was mixed with different gelatin solutions (0%, 10%, 20%, and 30%) at a powder-to-liquid ratio of 2 mg/mL using a conditioning mixer (ARE-250, Thinky, Tokyo, Japan). The mixture was then dried at room temperature for 12 h. The ratios of gelatin/calcium silicate in this study were approximately 0%, 5%, 10%, and 15% by weight (referred to as CSG0, CSG5, CSG10, and CSG15, respectively). After grinding the dried powder, the bulks were obtained by molding the specimens with an aspect ratio of 2:1 (6 mm in diameter × 12 mm in length for physicochemical tests and 6 mm in diameter × 3 mm in length for cell function tests). The specimens were molded in a cylindrical stainless steel mold under an applied pressure of 500 MPa for 1 min using a uniaxial press and soaked in deionized water at 60 °C for 1 h for hydrothermal processing prior to being dried at 60 °C for 2 days in an oven. The hydrothermal processing can promote the more complete hardening reaction between calcium silicate and water.

2.2. In Vitro Soaking. To evaluate the in vitro physicochemical activity, the specimens were immersed in a 37 °C, 30 mL SBF solution, equivalent to a specimen surface-to-volume ratio of 0.1 cm^{-1}, which was arbitrarily chosen to completely cover each surface of the specimen. The SBF solution, of which the ionic composition is similar to that of human blood plasma, consisted of 7.9949 g of NaCl, 0.3528 g of $NaHCO_3$, 0.2235 g of KCl, 0.147 g of K_2HPO_4, 0.305 g of $MgCl_2\cdot 6H_2O$, 0.2775 g of $CaCl_2$, and 0.071 of g Na_2SO_4 in 1000 mL of distilled H_2O and was buffered to a pH of 7.4 with hydrochloric acid (HCl) and trishydroxymethyl aminomethane (Tris, $(CH_2OH)_3CNH_2$).[7] All chemicals used were of reagent grade. The solution in the shaker water bath was not changed daily under a static condition.[11] After soaking for a specific time duration (15, 30, 90, and 180 days), specimens were removed from the vials and their properties were evaluated. Samples were removed from the vials and evaluated for compressive strength (CS) or were dried in an oven at 60 °C for the analysis of weight loss, phase composition, and morphology.

2.3. Phase Composition and Morphology. Phase analysis was performed using an X-ray diffractometer (XRD; Shimadzu XD-D1, Kyoto, Japan) operated at 30 kV and 30 mA at a scanning speed of 1°/min. Scanning electron microscopy (SEM; JEOL JSM-7401F, Tokyo, Japan) associated with energy dispersive spectroscopy (EDS) was used to characterize the microstructural and chemical analyses of the specimens. The surface morphology of the specimens were coated with gold using a JFC-1600 (JEOL, Tokyo, Japan) coater and examined by SEM operating in the lower secondary electron image mode (LEI) at 3 kV accelerating voltage. Three randomly chosen fields of the cross-sectional view were photographed of each specimen; thus, five specimens yielded 15 photos for each group.

2.4. Mechanical Properties. CS measurements were performed in an SBF solution at a cross head speed of 1 mm min^{-1} using an AG-1000E static mechanical testing machine (Shimadzu, Kyoto, Japan) with a 10 kN load cell. The CS value of each specimen was calculated as defined by the equation $CS = P/\pi r^2$, where P is the peak load (Newtons, N) and r is the radius (mm) of the specimen. The maximal compressive load at the point of failure was obtained from the recorded load-deflection curves. Eight specimens from each group were tested.

2.5. Weight Loss and pH Value. The degradation behavior was also determined by monitoring the weight change of the samples. The dried specimens were weighed until reaching a constant weight before (day 0) and after immersion using a four-digit balance (AE 240S, Mettler-Toledo AG, Greifensee, Switzerland). Eight repeated specimens were examined for each of the materials investigated at each time point. At each time point, the pH values of the SBF solutions were measured using a pH meter (SP-701, Suntex Instruments, Taipei, Taiwan). Eight measurements were used.

2.6. Cytotoxicity. The cytotoxicity of the bone grafts were evaluated by incubating the specimens with L929 mouse fibroblast cells (BCRC 60279, Hsinchu, Taiwan) for 12, 24, and 48 h. Prior to cell incubation, the specimens were sterilized by soaking each in a 75% ethanol solution and exposing to UV light for 2 h. The L929 cells were suspended in Dulbecco's Modified Eagle's medium (DMEM; Gibco, Langley, OK) containing 10% fetal bovine serum (FBS; Gibco) and 1% penicillin/streptomycin solution (Gibco). Cell suspensions (5×10^3 cells per well) were directly seeded over each of the specimens in a 96-well plate. The segmented polyurethane films containing 0.1% zinc diethyldithiocarbamate (RM-A) were used as positive standard reference materials, and a high-density polyethylene sheet (RM-C) was used as the negative standard reference material, based on ISO 10993-5. The two standard reference materials were purchased from Hatano Research Institute, Food and Drug Safety Center (Kanagawa, Japan). After the established L929-cell incubation period, the cytotoxicity was examined using the alamarBlue assay (Invitrogen, Grand Island, NY), which is based on the detection of mitochondrial activity. One microliter of alamarBlue solution and 100 μL of DMEM were added to each well followed by 2 h of incubation. After incubation, the solution in each well was transferred to a new 96-well ELISA plate. Plates were read in a Sunrise microtiter plate reader (Tecan Austria Gesell- schaft, Salzburg, Austria) at 570 nm with a reference wavelength of 600 nm. Optical density (OD) results were obtained from three separate experiments.

Table 1. Gene-Specific Primers

genes	sequences
actin (AC)	PCR product size: 539 (bp), *Homo sapiens*
forward	GTGGGCCGCCCTAGGCACCAG
reverse	CACTTTGATGTCACGCACGATTTC
collagen type I (COL I)	PCR product size: 255 (bp), *Homo sapiens*
forward	CCATGTGAAATTGTCTCCCA
reverse	GGGGCAAGACAGTGATTGAA
alkaline phosphatase (ALP)	PCR product size: 172 (bp), *Homo sapiens*
forward	TAGTTCCTGGTACCTCTGCTCC
reverse	CAGTTTCCTTTCCTGAATACCG
bone sialoprotein (BSP)	PCR product size: 297 (bp), *Homo sapiens*
forward	ATCCATGCCTAGTGGTGTGTTCT
reverse	ATCCAGCTTCCCAAGAAGGTAAC
osteopontin (OPN)	PCR product size: 210 (bp), *Homo sapiens*
forward	TTCAGGGTTATGTCTATGTTCATTC
reverse	CACACCACAAAAAGATAATCACAAC
osteocalcin (OC)	PCR product size: 573 (bp), *Homo sapiens*
forward	GTGCAGAGTCCAGCAAAGGT
reverse	CGATAGGCCTCCTGAAAGC
interleukin-10 (IL-10)	PCR product size: 187 (bp), *Homo sapiens*
forward	AGCCCCTTGAGAAACCTTATTG
reverse	AGTGTGTCACCCTATGGAAACAG
interleukin-1 (IL-1)	PCR product size: 229 (bp), *Homo sapiens*
forward	AGTCAGCTCTCTCCTTTCAGG
reverse	CTTGCCCCCTTTGAATAAAT
inducible NO synthase (iNOS)	PCR product size: 227−247 (bp), *Homo sapiens*
forward	ACGTCATAGTCTCTCTAAACCGTGC
reverse	GTGCTGACTGGAAATCTCAAGG

2.7. Primary Cell Culture. Human dental pulp cells were freshly derived from an intact caries-free premolar that was extracted for orthodontic treatment purposes, as previously described.[9] The patient gave informed consent. Approval from the Ethics Committee of the Chung Shan Medicine University Hospital was obtained. The tooth was split sagittally with a chisel, and the periodontal ligament tissue was then immersed in phosphate-buffered saline (PBS) solution. The pulp tissue was cut into fragments and immersed in DMEM containing 0.1% collagenase (Sigma) and 0.1% Dispase (Sigma) for 1 h. The pulp cells were collected from the medium by centrifugation at 1500 rpm for 5 min. The cell pellet was resuspended in DMEM containing 20% FBS, 100 units/mL penicillin G, and 100 mg/mL streptomycin in 5% CO_2 at 37 °C. Cells were subcultured by successive passaging at a 1:3 ratio. Cell cultures between the fourth and eighth passages were used. Pulp cell suspensions (2×10^4 cells per well) were directly seeded over each sterilized specimen, which was placed in a 24-well plate.

2.8. Cell Morphology. To observe cell morphology on the specimen surface, specimens were washed three times with PBS and fixed in 2% glutaraldehyde (Sigma) for 3 h after 3 h of seeding. The specimens were then dehydrated using a graded ethanol series for 20 min at each concentration and dried with liquid CO_2 using a critical point dryer device (LADD 28000; LADD, Williston, VT). The dried specimens were mounted on stubs, coated with gold, and viewed using SEM.

2.9. Cell Attachment and Proliferation. The reagent alamarBlue was used for real-time and repeated monitoring of cell attachment and proliferation. To assess the attachment, the cells were cultured for 3, 6, and 12 h. Cell proliferation was assessed on days 1, 3, and 7. Briefly, at the end of the culture period, the medium was discarded and the wells were washed twice with PBS. Each well was filled with 100 μL of solution at a ratio of 1:100 of alamarBlue to fresh medium and were incubated at 37 °C for 2 h. The solution in each well was transferred to a new 96-well tissue culture plate. Plates were read in a Sunrise Microtiter reader at 570 nm with a reference wavelength of 600 nm. The OD results were obtained in six independent measurements.

2.10. Cell Differentiation and the pH in Culture Medium. To evaluate the effect of gelatin amount on earlier cell differentiation, the alkaline phosphatase (ALP) activity assay was performed using a TRACP & ALP assay kit (Takara, Shiga, Japan) according to the manufacturer's instructions. The ALP catalyzes the hydrolysis of the colorless organic phosphate ester substrate, *p*-nitrophenyl phosphate (pNPP), to *p*-nitrophenol, a yellow product, and phosphate. To perform the assay, after incubation, the cells were washed with physiological saline (150 mM NaCl) and lysed in 50 μL of lysis buffer (1% NP40 in 150 mM NaCl). For measurement purposes, 50 μL of the substrate solution (20 mM Tris−HCl, 1 mM $MgCl_2$, 12.5 mM *p*-nitrophenyl phosphate, pH = 9.5) was added to each well and allowed to react at 37 °C for 30 min. The reaction was stopped by the addition of 50 μL of 0.9 N NaOH and read at 405 nm using a Sunrise Microplate Reader. The experiments were carried out in triplicate. The pH of the media was also monitored with an IQ120 miniLab pH meter (IQ Scientific Instruments, San Diego, CA). Triplicate measurements were used.

2.11. Gene Expression Analysis. Reverse transcriptase-polymerase chain reaction (RT-PCR) was used to determine gene expression in the human dental pulp cells cultured on the various specimens. The matrixes were washed with PBS on days 1, 3, 7, and 15, and the total RNA from the cells was isolated using Trizol (Invitrogen) according to the manufacturer's protocol. The total RNA concentration was quantified by the OD at 260 nm, and the OD260/OD280 ratio was calculated

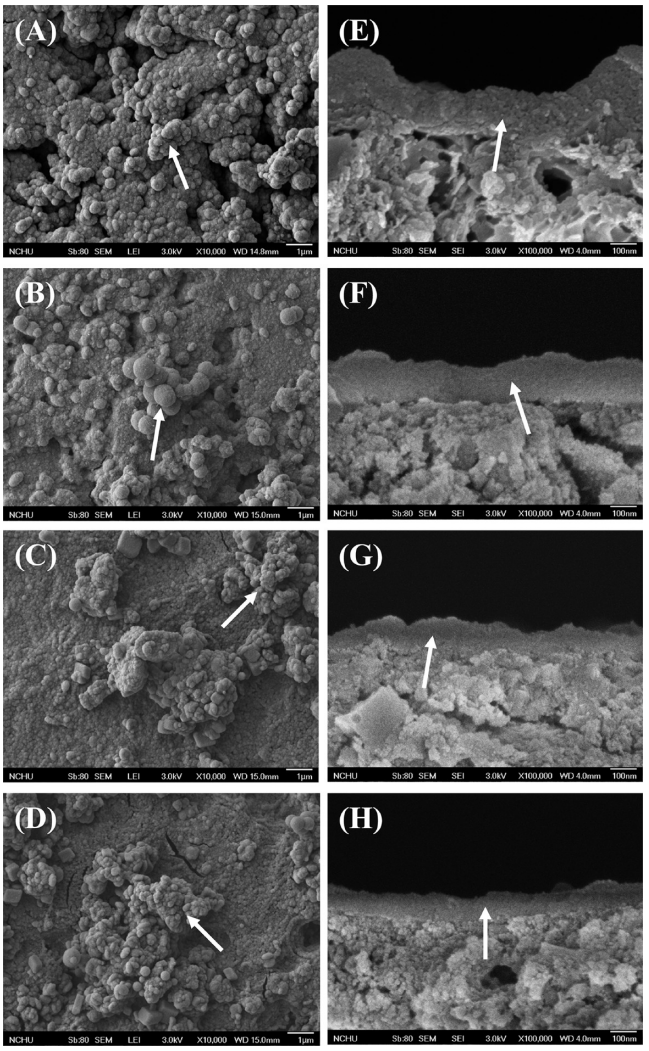

Figure 1. Surface (A−D) and cross-sectional (E−H) SEM micrographs of various bone grafts after soaking in an SBF solution for 1 day. (A, E) CSG0 control, (B, F) CSG5, (C, G) CSG10, and (D, H) CSG15. The arrows indicate the precipitated apatite spherulites or layers.

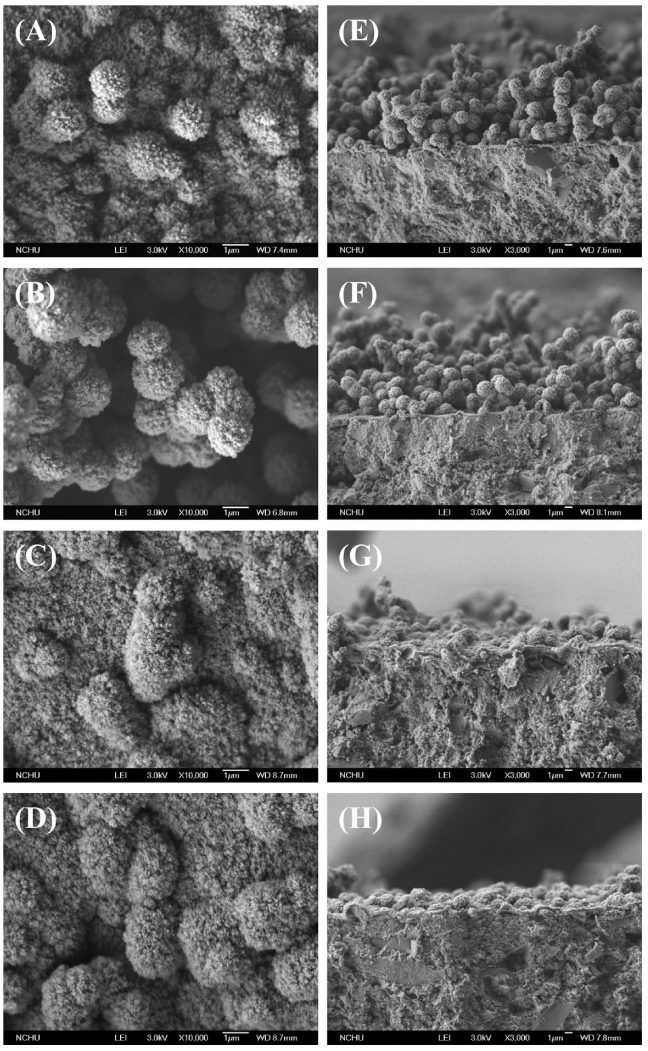

Figure 2. Surface (A−D) and cross-sectional (E−H) SEM micrographs of various bone grafts after soaking in an SBF solution for 180 days. (A, E) CSG0 control, (B, F) CSG5, (C, G) CSG10, and (D, H) CSG15.

using a Beckman DU640B spectrophotometer (Fullerton, CA). PCR primers were designed for various bone-formation genes: osteocalcin (OC), collagen type I (COL I), alkaline phosphatase (ALP), bone sialoprotein (BSP), and actin (AC). The primers for interleukin (IL)-1, IL-10, and inducible nitric oxide synthase (iNOS) are listed in Table 1. These primers were designed on the basis of published gene sequences (NCBI and PubMed). The mRNA was converted to cDNA using a thermal cycler (GeneAmp PCR System 9700, Applied Biosystems, Foster City, CA). Each PCR product was analyzed by separation with 2% agarose (in Tris−acetate−EDTA buffer) gel electrophoresis and visualized after ethidium bromide staining. The stained bands were photographed using a Syngene bioimaging system (Frederick, MD). For semiquantitative analysis of the genes, the photographed bands were analyzed with Scion Image software (Scion Corp., Frederick, MD), and the intensity of each band was normalized to that of AC. The semiquantitative analysis was carried out in three separate sets of experiments.

2.12. Immunofluorescence Staining. After incubation, unbound cells were washed with cold PBS, and the adherent cells were fixed in 4% paraformaldehyde (Sigma) for 30 min at room temperature and permeabilized with 0.1% Triton X-100 (Sigma) in PBS. Samples were blocked in PBS supplemented with 5% bovine serum albumin and washed three times with PBS-T (PBS contained 0.1% Tween 20). The cells were then incubated with mouse antihuman OC (Santa Cruz Biotechnology, Santa Cruz, CA) followed by a mixture of goat antimouse IgG antibodies conjugated to Alexa Fluor 488 (Invitrogen) and phalloidin conjugated to Alexa Fluor 546 (Invitrogen) for 90 min. The nuclei were stained with 300 nM 4′,6-diamidino-2-phenylindole (Invitrogen) in PBS for 90 min. After washing three times with PBS-T, the cells were viewed under indirect immunofluorescence using a Zeiss Axioskop2 microscope (Carl Zeiss, Thornwood, NY) at 200× magnification.

2.13. Statistical Analysis. One-way analysis of variance (ANOVA) was used to evaluate significant differences between means in the measured data. Scheffe's multiple comparison testing was used to determine the significance of the standard deviations in the measured data from each specimen under different experimental conditions. In all cases, results were considered statistically significant for a p-value of less than 0.05.

3. RESULTS

Broad face and cross-sectional SEM micrographs of various bone grafts after soaking in an SBF solution for 1 day are shown

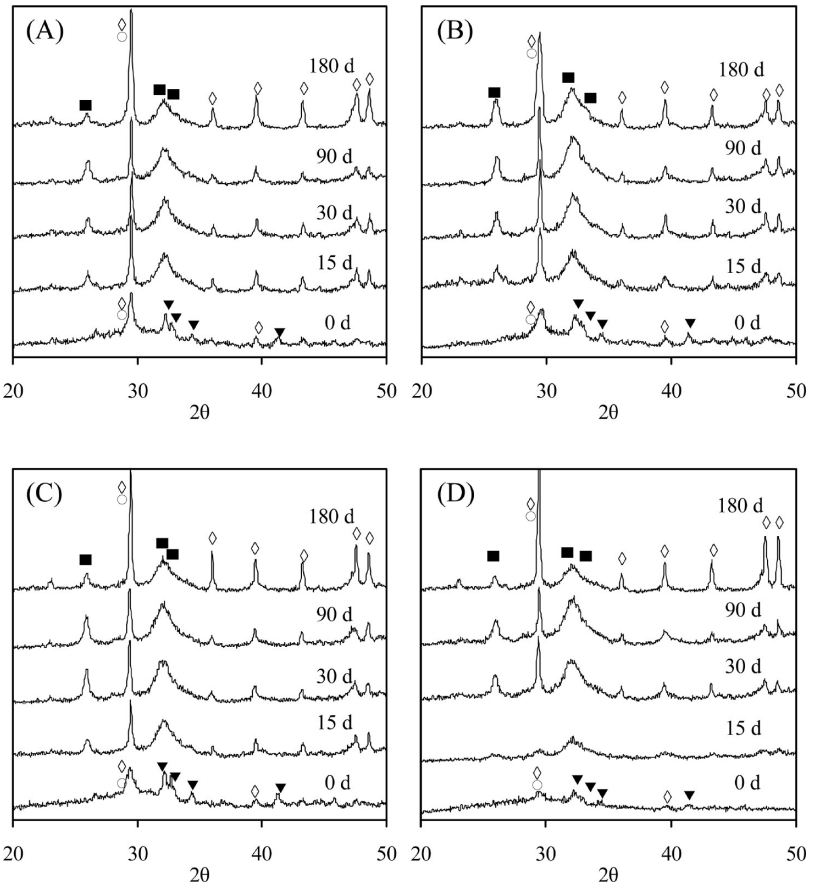

Figure 3. XRD patterns of various specimens before and after soaking in the SBF solution for predetermined time points. (A) CSG0 control, (B) CSG5, (C) CSG10, and (D) CSG15. (▼: β-Ca_2SiO_4; ◊: $CaCO_3$; ○: C−S−H; ■: apatite).

in Figure 1. It is clear that precipitation took place on all specimen surfaces, which were covered with clusters of precipitated apatite spherulites (Figure 1A−D). The precipitated apatite layers could be distinguished more clearly from the original surfaces in cross-sectional SEM micrographs due to the morphological differences, as indicated by the arrows in Figure 1E−H. The average thicknesses of the precipitated layers were approximately 220, 200, 160, and 100 nm for CSG0, CSG5, CSG10, and CSG15, respectively, which indicated a significant ($p < 0.05$) difference.

To further confirm that the observed layer was indeed ascribed to apatite precipitated from the SBF solution, SEM/EDS analyses were performed on the 1-day-immersed specimens, in addition to the XRD analysis. Ca/P ratios of the SBF-immersed specimens were 4.0, 4.5, 5.8, and 10.6 for CSG0, CSG5, CSG10, and CSG15, respectively, which significantly ($p < 0.05$) increased with increasing gelatin content.

It was of interest to immerse specimens in an SBF solution for extended time (up to 180 days) to investigate the variations in the activity and degradation of the composites. After soaking for 180 days, the surface morphology of the specimens was significantly altered in the presence of the etching-induced micropores on the apatite layer (Figure 2). It appears that during the immersion test dissolution of the surface had taken place. To further understand the etching effects, porosity measurements were conducted using a liquid displacement technique.[7] Before soaking in SBF, the porosities were 16%, 12%, 10%, and 11% for the specimens containing 0, 5, 10, and 15 wt % gelatin, respectively. On day 180, the porosities became 17%, 22%, 23%, and 28%, respectively. Significant differences ($p < 0.05$) between the porosities before and after soaking were found in the gelatin-containing composites.

The XRD patterns of all the prepared specimens revealed an obvious diffraction peak near $2\theta = 29.4°$, which corresponded to the calcium silicate hydrate (C−S−H) gel overlapping with calcite ($CaCO_3$) and incompletely reacted inorganic component phases of the β-dicalcium silicate (β-Ca_2SiO_4) (Figure 3). It is clear that the addition of gelatin resulted in the lower peak intensities of the C−S−H, $CaCO_3$, and β-Ca_2SiO_4 phases. After soaking in the SBF solution, broad and diffuse peaks at $2\theta = 25.9°$ and 31.8−32.9° clearly appeared in the resulting XRD patterns, which may be ascribed to the characteristic peaks of apatite. Interestingly, the $CaCO_3$ phases increased with the increasing soaking time. In short, the four specimens showed the same XRD pattern evolution during the soaking time.

The compressive strength values of the prepared specimens were 86, 105, 142, and 98 MPa for CSG0, CSG5, CSG10, and CSG15, respectively. The results revealed that all four types of bone grafts gradually lost their strength with an increased soaking time (Figure 4). Of note, the strength of CSG15 declined significantly from the prepared strength of 98 to 39 MPa after soaking for 180 days ($p < 0.05$), a reduction of approximately 60%. The CSG5 and CSG10 composites significantly ($p < 0.05$) lost 30% and 47% in compressive strength, respectively, after 180 days of soaking. In contrast, the CSG0 control decreased by about 11%, which was not significantly different ($p > 0.05$) than its strength as prepared.

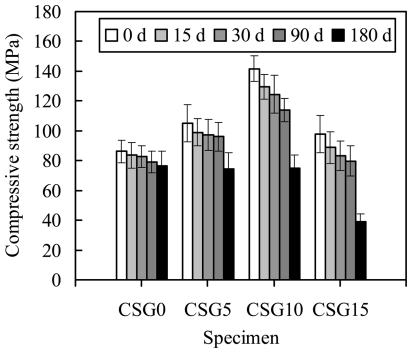

Figure 4. Compressive strength of the specimens before and after soaking in an SBF solution for predetermined time durations.

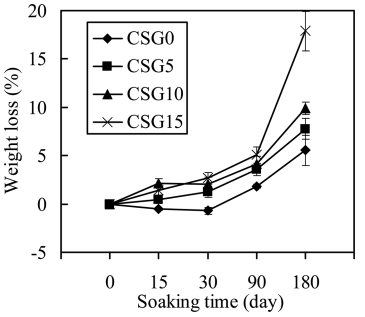

Figure 5. Weight loss of the specimens before and after soaking in an SBF solution for predetermined time durations.

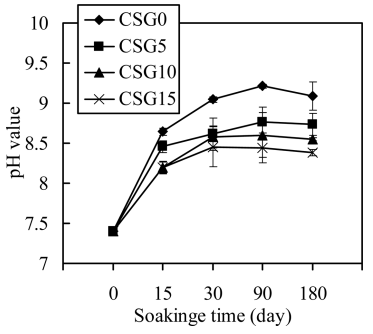

Figure 6. Variations in the pH of the SBF solution during soaking.

The effect of the soaking time on the changes in the weight of the bone graft specimens are presented in Figure 5. After soaking for 15 days, gelatin-containing composites showed a small amount of weight loss (~2%), whereas the CSG0 control gained weight. All the specimens exhibited an increased weight loss with an increase in the soaking time, reaching a weight loss of up to about 1−5% after 90 days depending on the type of specimen. At the end of the soaking experiment (180 days), weight loss of approximately 6%, 8%, 10%, and 18% were observed for CSG0, CSG5, CSG10, and CSG15, respectively, which indicated a significant difference ($p < 0.05$).

While soaking in the SBF solution, all bone grafts caused the pH of the solution to increase during the first 15 days, as shown in Figure 6. By day 30, the pH of the solution approached a steady state value ranging from 8.4 to 9.0 depending on the type of bone grafts. A greater amount of gelatin in the composite produced a lower pH value of the SBF solution. On day 180, the pH of the solution containing CSG0 (pH 9.1) was significantly ($p < 0.05$) higher than the pH of the solution containing the gelatin-containing composites (pH 8.4−8.7).

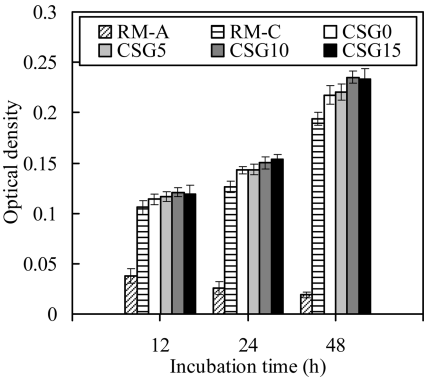

Figure 7. Cytotoxicity of various test samples seeded with L929 cells at various time points. RM-A and RM-C were used as the positive control and negative control, respectively.

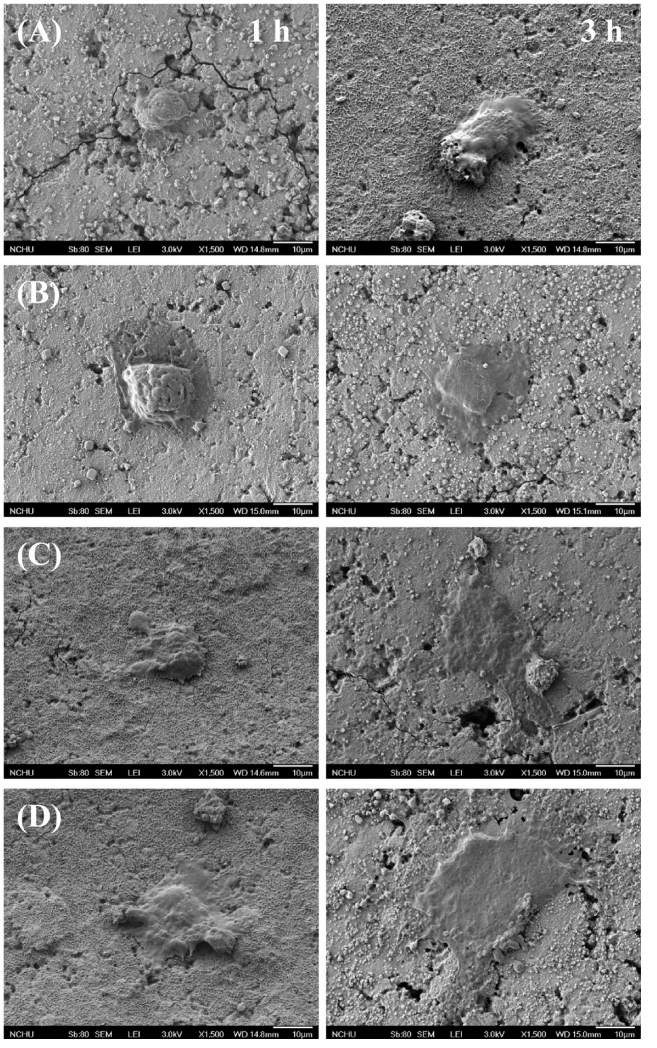

Figure 8. SEM images of pulp cells cultured on the (A) CSG0 control, (B) CSG5, (C) CSG10, and (D) CSG15 surfaces for 1 h (left) and 3 h (right).

The results of the alamarBlue assay for cytotoxicity are shown in Figure 7. The cells on the positive control (RM-A) showed a high degree of cytotoxicity with an increase in the culture time while OD values decreased. In contrast, the negative control (RM-C) exhibited an increased OD level of mitochondrial activity with an increasing culture time. When the cells were seeded on different bone grafts, no depression of cellular activity occurred. More importantly, the absorbance values of all the tested bone grafts were significantly ($p < 0.05$) higher than those obtained from the negative control after 24 and 48 h of culture.

Figure 8 shows the morphology of human dental pulp cells attached to various specimens after 1 and 3 h of culture. At hour 1, pulp cells attached to the CSG10 and CSG15 surfaces were spread out, but the shape of cells attached to the CSG0 and CSG5 surfaces was round. When cultured for 3 h, the SEM images revealed that the cells cultured on specimens with a higher content of gelatin (CSG10 and CSG15) were flat with an intact, well-defined morphology and extending filopodia, which is indicative of cellular adhesion.

Figure 9 shows that a higher attachment of pulp cells was observed for the gelatin-containing specimen surfaces than that for the surface of the control specimen after 3 h of culture. CSG15 indicated an increase of approximately 13% ($p < 0.05$) in the OD value compared to the CSG0 control during the initial 12 h incubation. Similarly, cell proliferation was notably higher in the gelatin-containing specimens than the cells in the control. Moreover, the optical density values increased with an increase in the culture time.

One possibility is that this trend in the elevated pH value, caused when soaking materials in an SBF solution, would be expected with cell culture. Figure 10A shows the variations of the pH in culture medium during the culture interval of pulp cells seeded on the specimens. It can be clearly seen that the pH values significantly ($p < 0.05$) increased from initially 7.3 to 7.6−7.8 after 1 h of assay, reaching a higher value after 3 days. The pH revealed a decrease with an increased gelatin amount of the composites. There are significant ($p < 0.05$) differences in extracellular pH between CSG0 control and CSG15 at all incubation times.

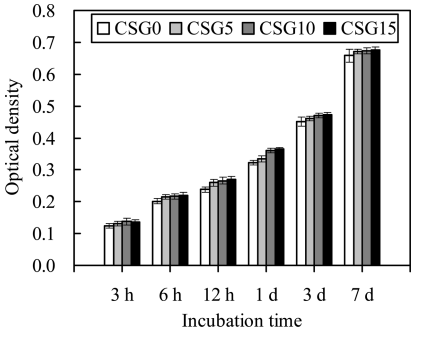

Figure 9. AlamarBlue assay of dental pulp cells cultured on the specimens to reveal cell attachment and proliferation at various time points.

The intracellular ALP level was measured to observe the functional activity of cells, as shown in Figure 10B. The intracellular ALP level increased with the gelatin content of the composites at all incubation times. On day 3, a significant 15% increment ($p < 0.05$) in ALP level was measured for CSG15 compared to the CSG0 control. The increment became 12% and 9% after 7 and 15 days, respectively, together with the significant ($p < 0.05$) differences.

Changes in the phenotype marker expression of the pulp cells for varying culture durations are shown in Figure 11. AC was used as an internal control and was produced at a comparable level in control cells and in the cells grown on the test specimens. Collagen is the major constituent of organic bone matrix, and its expression was similar in the control and experimental groups at all culture time points (Figure 11A). On day 1, the gene expression levels of all osteogenic differentiation biomarkers including ALP, BSP, OPN, and OC were not detected. ALP expression peaked in the gelatin-containing cells after 7 days of incubation, which was significantly higher ($p < 0.05$) than in cells adhered to the CSG0 control, but the expression was all down-regulated after 15 days of culture except in the control (Figure 11B). In contrast, BSP secretion on days 3, 7, or 15 was enhanced in cells cultured on the higher gelatin-containing specimen surfaces compared to those on the lower gelatin specimens (Figure 11C). Similar to BSP, as the content of the gelatin increased, the level of OPN increased (Figure 11D). OC production was greatest in the pulp cells cultured on CSG10 and CSG15 compared to the cells on the other two specimens (Figure 11E).

To further investigate the effects of gelatin on pulp cell functions, OC was analyzed using immunofluorescence microscopy after treatment with fluorescently labeled IgG (Figure 12). Visual examination showed that pulp cells seeded on the CSG10 and CSG15 surfaces exhibited comparatively higher fluorescence intensity than on the control surface on day 7. In addition, many reactive sites for OC were clearly found in regions of cells, particularly for the higher gelatin content specimens on day 15.

This study also addressed the role of gelatin on the immune expression of IL-1 and iNOS in human dental pulp cells. IL-1 (Figure 13A) and iNOS (Figure 13B) production on day 1 were higher in the pulp cells grown on the CSG0 control compared to all the other gelatin-containing composites. Significant differences ($p < 0.05$) in IL-1 and iNOS expression were detected between the bone grafts at all time points. With increasing

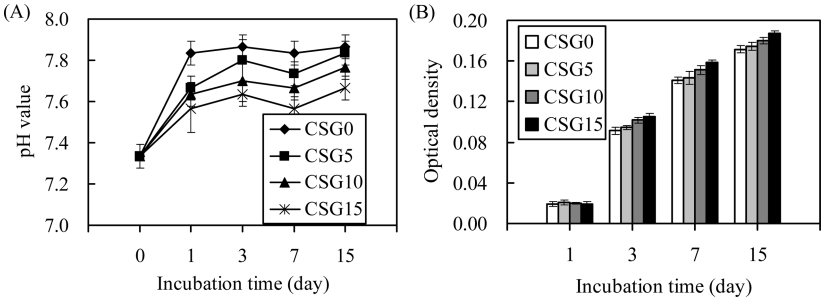

Figure 10. (A) Variations of the pH in culture medium and (B) ALP assay on the pulp cells presented as optical density for cell differentiation on various test groups.

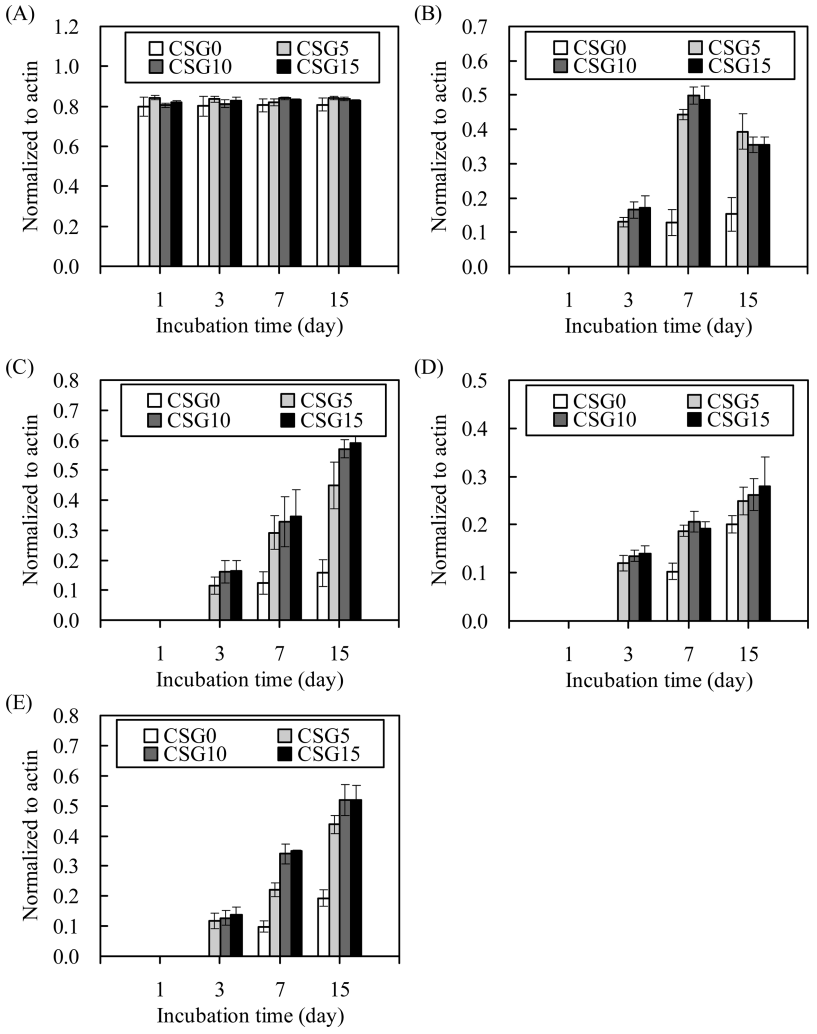

Figure 11. Osteogenic expression levels of the pulp cells cultured on the specimens at various time points. The intensity of each amplified cDNA band was semiquantified and normalized to that of actin. COL I = collagen I, ALP = alkaline phosphatase, BSP = bone sialoprotein, OPN = osteopontin, and OC = osteocalcin. (A) COL I, (B) ALP, (C) BSP, (D) OPN, and (E) OC.

incubation time, the two pro-inflammatory cytokines had a decreased expression. In contrast, pulp cells grown on CSG15 had the highest level of anti-inflammatory cytokine IL-10 expression among all of the specimens (Figure 12C), resulting in a significant difference ($p < 0.05$) compared to the other specimens.

4. DISCUSSION

The objective of this study was to develop synthetic bone analogs with improved mechanical and osteoconductive properties based on calcium silicate and gelatin. Such a system would combine the benefits of composite properties, resorbability (the ability to be replaced by native bone tissue), and osteoconductivity (the ability to induce bone growth). Furthermore, the evolution of mechanical properties due to the resorbability of gelatin can provide a progressive load transfer from the implant to the bone during healing, thereby eliminating stress shielding.[12,13] New composite systems also open the possibility of forming calcium silicate-based implant materials, especially in prefabricated forms, with a broad range of compositions and properties.

Exposure of a material surface to SBF promotes the precipitation of a "bone-like" apatite layer, which may support the material's ability to integrate into living tissue. After soaking in an SBF solution for 1 day, the formation of apatite spherulites was found on all bone graft surfaces, which indicates high bioactivity of the current bone grafts. However, there were significant differences in the thickness of the precipitated apatite layers formed on the specimens examined. The apatite-forming ability of the four bone grafts seemed to be dependent on the gelatin content of the composites. The presence of gelatin delayed the apatite precipitation rate. Nevertheless, all the bone grafts showed a strong tendency for "attracting" apatite precipitate to their surfaces, as evidenced by the Ca/P molar ratio. The much higher Ca/P ratio (compared to the 1.67 stoichiometric Ca/P ratio of apatite) on 1-day-immersed surfaces was not surprising due to the fact that a large quantity of calcium originating from the underlying specimens was detected. The lower Ca/P ratio on the surface of the CSG0 control without gelatin was possibly due to the faster apatite precipitation rate, consistent with the thickness of the precipitated layer. The in vitro bioactivity of the SiO_2−CaO-based materials indicates that the presence of PO_4^{3-} ions in the composition is not an essential requirement for the development of an apatite layer, which consumes the calcium and phosphate ions. This is because PO_4^{3-} ions originate from the in vitro assay solution.[11,14]

An increase in the pH of SBF at different time intervals was attributed to the release of $Ca(OH)_2$,[15,16] which is conducive for the formation of apatite precipitation. The results of the higher pH value in the CSG0 control-immersed SBF paralleled the apatite precipitation rate.

The bone graft substitutes in the reconstruction of hard, load-bearing tissues should have sufficient mechanical strength for retaining their structure after implantation. The biostability of many bone implants depends on factors such as strength, absorption at the material interface, and chemical degradation.[17] One concern is whether the incorporation of gelatin may result in biodegradation of the mechanical properties of bone graft substitutes. Indeed, the added gelatin played a crucial role in defining the properties of the composite materials. Gelatin resulted in a decreased strength of the composite bone grafts after soaking in SBF, particularly for 180 days. Among the composites studied, the 10 wt % gelatin-containing calcium silicate (CSG10) exhibited the maximum value of the initial compressive strength (about 142 MPa), which was strong enough to be used in load-bearing sites of bone tissue.[7] The high initial strength was because gelatin served as a "glue" to fuse the particles together, which in turn reduced the porosity and modified the stress acting on the calcium silicate ceramic.[7] The measured strength values of the immersed CSG10 were in the range of 75−130 MPa with significant differences ($p < 0.05$) among the various soaking intervals. In contrast, the CSG0 control did not change with duration of soaking time (within 10%) and was significantly different from strength degradability of gelatin-containing composites. Hence, the decreased strength was mainly a result of the degradation of water-soluble gelatin, which led to the formation of a porous structure, in concurrence with the results of the porosity. Water/ions from the solution infiltrate the inner portion of the materials through structural imperfections such as pores and defects and come into contact with the deeper portion of the materials, which results in a weakened structure.[11] Additionally, the addition of gelatin can enhance the water absorption of composites, which could lead to a reduced retention of the mechanical properties of gelatin−calcium silicate composites in an SBF solution. The other important reason for the decreased strength in SBF was possibly due to the quick degradation on weight, in particular for 15 wt % gelatin-containing composites after 180 days, as discussed later. Nevertheless, Martin et al. suggested that strength was most needed in the early stages of implantation, because the strength of bone implants increases over time once new bone begins to grow and adhere to the materials.[18] Hence, the present study developed composite bone grafts to provide at least the necessary early stage strength.

The degradation rates of all specimens were also characterized by their weight loss in SBF. The degradation of the current bone graft systems was a slow process with the exception of CSG15, and the degree of the degradation was time dependent. When soaked in SBF, the three gelatin-containing bone graft systems were associated with a relatively small degree of weight loss of about 2% after a 30-day soaking time; the CSG0 control even exhibited a weight increase. The few changes in sample weight

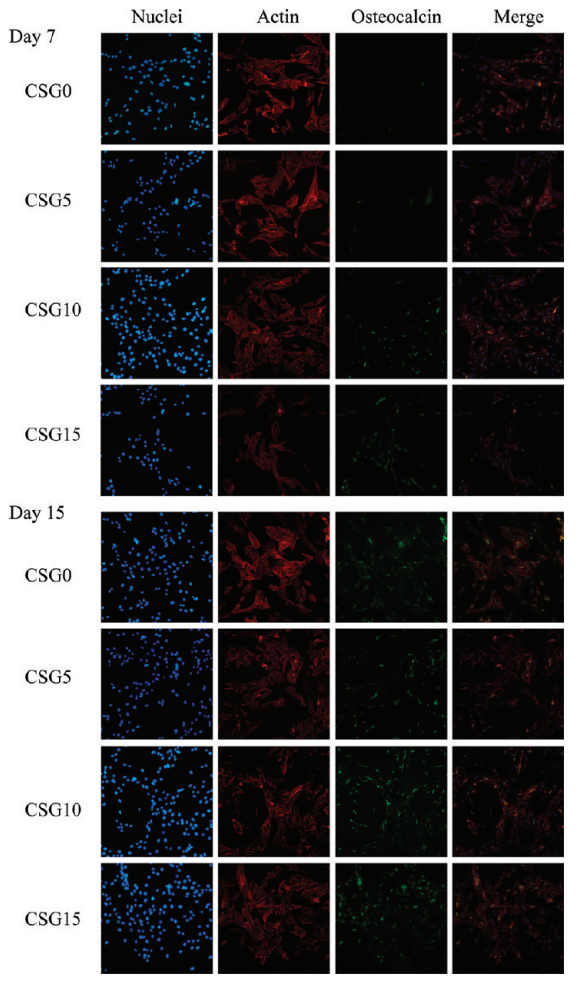

Figure 12. Immunofluorescence images of nuclei (blue), actin (red), and osteocalcin (green) in the pulp cells cultured on the four specimens on days 7 and 15 (original magnification ×200).

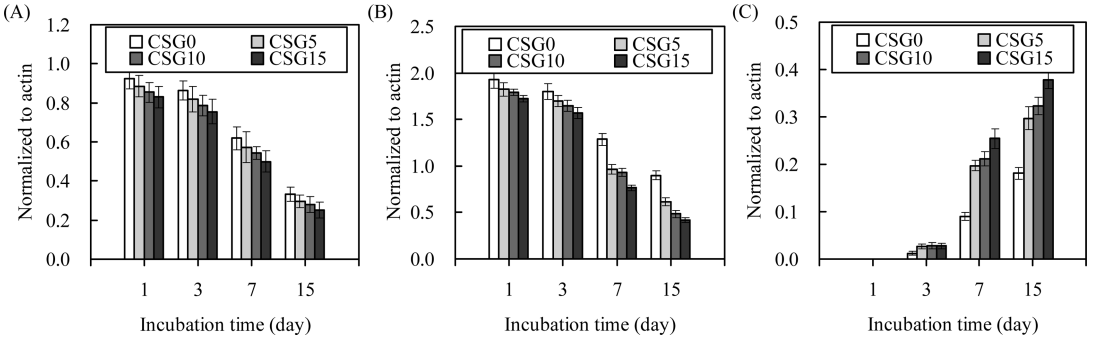

Figure 13. (A) IL-1, (B) iNOS, and (C) IL-10 responses in the pulp cells cultured on the specimens. The mRNA levels of IL-1, iNOS, and IL-10 were determined using RT-PCR and normalized to the corresponding actin mRNA levels.

may be explained by the formation of apatite, which was consistent with the morphology results. The four specimens continued to dissolve without stopping accompanied by continued weight loss after 90 days. This may be due to the release of soluble fractions (mainly gelatin). Because gelatin is biocompatible and has been classified as a bioresorbable material,[19] its presence or dissolution is not expected to cause biological problems. Immersed CSG15 reached its maximal weight loss of 18% on day 180. It is important to note that 10 wt % gelatin (CSG10) led to a weight loss of 10% even after soaking in an SBF solution for 180 days. Moreover, the trend in weight loss of gelatin-containing composites was similar to the changes in the compressive strength. High physiochemical activity and low degradability were the characteristics of the present SiO_2−CaO-based material, which are of utmost importance and a necessity for successful results of bone graft substitutes for vertebroplasty applications.[20] The designed composites were expected to have an optimal mechanical performance, a controllable degradation rate, and eminent bioactivity, which will be of great importance for bone remodeling and growth. However, the degradation rate and mechanical strength may be improved to support large defect sites for long-lasting and permanent implantation applications.

One issue necessary to be concerned is the effect of the in vitro protocol on the bioactivity and degradation of the materials. In order to simulate the constant circulation of physiological fluids in the body, either continuous exchange or periodical changing (dynamic condition) of SBF may be a more effective assay which makes more precise predictions of the bioactivity and degradation than a static assay (the lack of SBF exchange) used in the present study. In a study by Izquierdo-Barba et al., remarkable variations in ionic concentration and pH of solution were detected after a few minutes of soaking for static assay.[21] Contrary to the findings, exchange of solution could maintain SBF ionic concentration and pH almost constant and close to plasma. However, the static assay was a simpler method in terms of many sample numbers and long-term soaking compared to the dynamic assay. Nevertheless, the differences in the degradation rate and the subsequent changes in compressive strength between the two assays are worth investigating.

Regarding cytotoxicity, it is certainly evident that no bone grafts showed signs of cytotoxicity. Cell viability and functions associated with a bone graft are closely related to the physical, chemical, and biological characteristics of the materials used. Cell attachment, spreading, and shape are important modulators of cellular function.[22,23] The pulp cells transformed from a rounded morphology, characteristic of initial attachment to a discoid shape within 1 h. The close proximity of the pulp cells to the higher gelatin content composite indicated a favorable interaction between the cells and the materials. Thus, the beneficial effects of gelatin on cellular functions may be due to the role of adhesion.[19]

To elucidate the effects of gelatin on osteogenic activity, the biological functions of pulp cells cultured on various gelatin-containing specimens were evaluated. The number of cells initially attached was different between the bone grafts with and without gelatin. Cell attachment and proliferation increased after the incorporation of either 10% or 15% gelatin to the control, although there was no significant difference ($p > 0.05$) after Scheffe's multiple comparison testing. When gelatin was present on the specimen surfaces, cellular attachment took place rapidly, possibly via interactions between the functional OH, COOH, and NH_2 groups of the gelatin and the integrins.[19] The interactions may consequently influence the spreading, proliferation, and differentiation of the cells. Cell-differentiation studies, like cell-proliferation assay results, showed a significant impact of gelatin, with an emphasis on the importance of material composition. ALP activity was seen to increase up to day 15 on the materials, with enzyme activity increasing with amount of gelatin. It is generally accepted that an increase in the specific activity of ALP in bone cells reflects a shift to a more differentiated state.[24] ALP enzyme activity is also associated with bone formation, and it is produced in high levels during the bone formation phase.[25]

A synchronized sequence of genes must be activated in the osteoblasts so that they undergo cell division and then synthesize an extracellular matrix that is capable of mineralizing to become bone. The cellular response of osteoblasts to foreign materials is genetically controlled. Osteoblast differentiation is generally accompanied by ALP expression, the production of BSP, OPN, OC, and COL I, and in vitro mineralization. There were no significant differences in COL I expression among the four bone grafts. The secretion of ALP from pulp cells was initiated earlier for cultures on the gelatin-containing composite surfaces than on the control surface. ALP appears to play a crucial role in the initiation of matrix mineralization, and ALP gene expression is down-regulated after the start of mineralization, as shown in all gelatin-containing composites on day 15. Our results were consistent with previous reports.[9,26] As an example, ALP gene expression of human umbilical cord stem cells on calcium phosphate−chitosan cement achieved a higher level on day 4 and then slightly decreased on day 8.[26] ALP gene expression was coincident with ALP enzyme activity on days 3 and 7 of incubation. On the contrary, after 15 days, this profile of the translated protein, measured here as ALP enzymatic activity, differed from the expression profile observed at the mRNA level. A factor may account for disparities between measured gene expression and enzyme activity levels on day 15. The translational machinery can translate a given mRNA many times into polypeptides which are then transformed into active enzyme.[27] Thus, this would lead to a profile in which there is an initial increase in mRNA that is lagged by an enzyme activity. In a word, degradation of the mRNA could begin at a certain time point and enzyme activity would reach a plateau. The potential explanation for the low number of increments seen in ALP enzyme activity results with incubation time may be an indicator of the cell progressing in mineralization.

OC is the most abundant noncollagenous bone-matrix protein characteristic of osteoblast synthetic function. The synthesis of OC is recognized at the late stage in osteoblast differentiation, and its expression increases rapidly as mineralization increases.[28] BSP is specific to mineralized tissues, and strong mRNA expression of BSP is observed in fully differentiated osteoblasts associated with the initial formation of bone, as is the distribution of OC.[29] OPN is one of the major phosphoproteins of mammalian bone, and its expression occurs later during bone formation.[30] Pulp cells on the gelatin-containing composites showed significantly increased BSP, OPN, and OC expression levels with increased culture time compared to the control without gelatin. Likewise, similar results were obtained after immunofluorescence staining for the OC biomarker. OC protein synthesis was most evident in the composite with the higher gelatin amount, which stained much more intensely than the others. The results of the current study consistently indicated that the presence of gelatin was effective in supporting the proliferation of pulp cells and actively stimulating a biological response in these cells through the production of bone-specific proteins. The presence of gelatin provided a favorable

environment for pulp cells, resulting in a large amount of mineralized tissue formation.

In the current study, immunocompatibility was evaluated by measuring the expression of IL-1, iNOS, and IL-10. IL-1 is the first "immune" cytokine positively identified to be involved in the control of bone turnover and stimulates the proliferation of osteoclast precursors. It is also a typical example of multifunctional cytokines involved in the regulation of immune responses, hematopoiesis, and inflammation.[31] iNOS is only expressed in responses to inflammatory stimuli. IL-1 causes activation of the iNOS pathway in bone cells.[32] It was found that both IL-1 and iNOS expression of pulp cells on the bone grafts decreased with increasing incubation time. Most importantly, the lowest levels of the pro-inflammatory cytokine IL-1 and iNOS were expressed by pulp cells cultured on the specimen with the highest gelatin content at all culture time points. Interestingly, Scheffe's multiple comparison testing indicated that gelatin-containing specimens had significantly ($p < 0.05$) higher IL-10 values than the CSG0 control at all culture time points, with the exception of the 1-day expression of which there was no reaction. The greater the amount of gelatin in the bone grafts, the more iNOS and IL-1 expression levels were inhibited and the more IL-10 was activated.

In addition to the role of gelatin in cell functions, another point of interest in the changes of the pH is its relation with the cell behavior. Cellular mechanisms involved in bone formation and resorption may be responsive to the acid−base balance. During bone formation, the pH of the bone interstitial fluid may shift to an alkaline pH and during resorption to an acid pH.[33] An alkalinization of the extracellular medium with the bone grafts rather than the normal pH (7.4) during cell culture was indeed determined. Alkalinization of the medium caused by calcium silicate-based materials was not unexpected because reactions which the material underwent in physiological solutions involved a mandatory disappearance of protons.[34] More importantly, the alkalinization of the medium is relevant to the enhancement of osteoblastic function, since it is accompanied by a shift in the intracellular pH in the same direction in the culture systems of osteoblastic clone cells and cell lines.[35] Ramp et al. tested the effects of medium pH ranging from 6.8 to 8.2 on calvariae, tibiae, and osteoblast-like cells from chick embryos.[33] As medium pH was increased, glycolysis, collagen synthesis, and ALP activity increased, while Ca efflux decreased. However, no effect of pH was seen on mitochondrial activity, phosphate efflux, or cell number or proliferation. In contrast, Leblebicioglu et al. showed an impairment of chemotaxis at pH 7.7 and 8.2 but found no change at pH 6.7.[36] Lardner reported that increasing the ambient pH beyond 7.6 produced a significant decrease in cell movement, with complete and irreversible inhibition of motility occurring at pH 7.9.[37] Therefore, an excessive abnormal pH (alkaline) might damage cell functions. In the present study, the effect of increasing the amount of gelatin was to drive the entire culture system toward a normal pH; efforts to elucidate these relationships with cell functions are worth making. On the other hand, the effects of acid−base balance on the inflammatory response are highly relevant to clinical medicine. Production of inflammatory cytokines, as well as DNA-binding of transcription factors in their control pathways, appears to be sensitive to extracellular pH as well.[38] Raising the pH of culture medium enhanced immune resistance.[37] Taken together, it is postulated that the beneficial effect of gelatin-containing composites on in vitro cell growth might be due to some extent to alkalinization.

5. CONCLUSIONS

Highly active composite bone graft substitutes with high initial strength and osteogenic activity were developed, consisting of calcium silicate and gelatin. All composite bone grafts formed "bone-like" apatite spherulites in an SBF solution on the initial day, although the incorporation of gelatin was likely to reduce formation of apatite in vitro. The presence of gelatin enhanced the in vitro degradability of calcium silicate−gelatin but promoted the osteogenic activity of the pulp cells. The pulp cells cultured on gelatin-enriched materials exhibited higher levels of osteogenic differentiation biomarkers, such as BSP, OPN, and OC. Moreover, gelatin effectively inhibited iNOS and IL-1 expression and activated IL-10 expression. Taking the high initial mechanical strength and biological functions into account, the 10 wt % gelatin−calcium silicate composites appear to be promising for the use in load-bearing applications such as dental and orthopedic repair. More importantly, it is more suitable for a small bone defect or fast healing trauma site.

AUTHOR INFORMATION

Corresponding Author

*Tel: 886-4-24718668 ext. 55529. Fax: +886-4-24759065. E-mail: sjding@csmu.edu.tw.

ACKNOWLEDGMENT

This work was supported by National Science Council of the Republic of China under the Grant No. NSC 98-2221-E-040-006-MY3.

REFERENCES

(1) Moore, W. R.; Graves, S. E.; Bain, G. I. *ANZ J. Surg.* **2001**, *71*, 354–361.

(2) Alves, N. M.; Leonor, I. B.; Azevedo, H. S.; Reis, R. L.; Mano, J. F. *J. Mater. Chem.* **2010**, *20*, 2911–2921.

(3) Shie, M. Y.; Ding, S. J.; Chang, H. C. *Acta Biomater.* **2011**, *7*, 2604–2614.

(4) Heinemann, S.; Heinemann, C.; Ehrlich, H.; Meyer, M.; Baltzer, H.; Worch, H.; Hanke, T. *Adv. Eng. Mater.* **2007**, *9*, 1061–1068.

(5) Chen, C. C.; Lai, M. H.; Wang, W. C.; Ding, S. J. *J. Mater. Sci. Mater. Med.* **2010**, *21*, 1057–1068.

(6) Ding, S. J.; Shie, M. Y.; Hoshiba, T.; Kawazoe, K.; Chen, G.; Chang, H. C. *Tissue Eng. A* **2010**, *16*, 2343–2354.

(7) Ding, S. J.; Wei, C. K.; Lai, M. H. *J. Mater. Chem.* **2011**, *21*, 12793–12802.

(8) Kim, S. J.; Min, K. S.; Ryu, H. W.; Lee, H. J.; Kim, E. C. *J. Endod.* **2010**, *36*, 1326–31.

(9) Chen, C. C.; Shie, M. Y.; Ding, S. J. *Int. Endod. J.* **2011**, *44*, 836–842.

(10) Ding, S. J.; Shie, M. Y.; Wang, C. Y. *J. Mater. Chem.* **2009**, *19*, 1183–1190.

(11) Chen, C. C.; Wang, W. C.; Ding, S. J. *J. Biomed. Mater. Res. B: Appl. Biomater.* **2010**, *95*, 456–465.

(12) Durucan, C.; Brown, P. W. *Adv. Eng. Mater.* **2001**, *3*, 227–231.

(13) Barralet, J. E.; Gaunt, T.; Wright, A. J.; Gibson, I. R.; Knowles, J. C. *J. Biomed. Mater. Res.* **2002**, *63*, 1–9.

(14) Chen, C. C.; Ho, C. C; Chen, C. H.; Wang, W. C.; Ding, S. J. *J. Endod.* **2009**, *35*, 1554–1557.

(15) Zhao, W.; Chang, J.; Wang, J.; Zhai, W.; Wang, Z. *J. Mater. Sci. Mater. Med.* **2007**, *18*, 917–923.

(16) Gandolfi, M. G.; Taddei, P.; Tinti, A.; Prati, C. *Int. Endod. J.* **2010**, *43*, 917–929.

(17) Yang, S.; Leong, K. F.; Du, Z.; Chua, C. K. *Tissue Eng.* **2001**, *7*, 679–689.

(18) Martin, R. B.; Chapman, M. W.; Holmes, R. E.; Sartoris, D. J.; Shors, E. C.; Gordon, J. E.; Heitter, D. O.; Sharkey, N. A.; Zissimos, A. G. *Biomaterials* **1989**, *10*, 481–488.
(19) Ding, S. J.; Shie, M. Y. *Adv. Eng. Mater.* **2011**, *13*, B246–B255.
(20) Heini, P. F.; Berlemann, U. *Eur. Spine J.* **2001**, *10*, S205–213.
(21) Izquierdo-Barba, I.; Salinas, A. J.; Vallet-Regí, M. *J. Biomed. Mater. Res.* **2000**, *51*, 191–199.
(22) Wu, C. C.; Yuan, C. Y.; Ding, S. J. *Surf. Coat. Technol.* **2011**, *205*, 3182–3189.
(23) ter Brugge, P. J.; Dieudonne, S.; Jansen, J. A. *J. Biomed. Mater. Res.* **2002**, *61*, 399–407.
(24) Malaval, L.; Liu, F.; Roche, P.; Aubin, J. E. *J. Cell. Biochem.* **1999**, *74*, 616–627.
(25) Sabokbar, A.; Millett, P.; Myer, B.; Rushton, N. *Bone Miner.* **1994**, *27*, 57–67.
(26) Zhao, L.; Weir, M. D.; Xu, H. K. K. *Biomaterials* **2010**, *31*, 3848–3857.
(27) Glanemann, C.; Loos, A.; Gorret, N.; Willis, L. B.; O'Brien, X. M.; Lessard, P. A.; Sinskey, A. *J. Appl. Microbiol. Biotechnol.* **2003**, *61*, 61–68.
(28) Mizuno, M.; Kuboki, Y. *J. Biochem.* **2001**, *129*, 133–138.
(29) Hunter, G.; Goldberg, H. A. *Proc. Natl. Acad. Sci. U.S.A.* **1993**, *90*, 8562–8565.
(30) Chen, J.; Shapiro, H. S.; Sodek, J. *J. Bone Miner. Res.* **1992**, *7*, 987–997.
(31) Akira, S.; Hirano, T.; Taga, T.; Kishimoto, T. *FASEB J.* **1990**, *4*, 2860–2867.
(32) van't Hof, R. J.; Ralston, S. T. *Immunology* **2001**, *103*, 255–261.
(33) Ramp, W. K.; Lenz, L. G.; Kaysinger, K. K. *Bone Miner.* **1994**, *24*, 59–73.
(34) Silver, I. A.; Deas, J.; Erecińska, M. *Biomaterials* **2001**, *22*, 175–185.
(35) Ehara, A.; Ogata, K.; Imazato, S.; Ebisu, S.; Nakano, T.; Umakoshi, Y. *Biomaterials* **2003**, *24*, 831–836.
(36) Leblebicioglu, B.; Lim, J. S.; Cario, A. C.; Beck, F. M.; Walters, J. D. *J. Periodontol.* **1996**, *67*, 472–477.
(37) Lardner, A. *J. Leukocyte Biol.* **2001**, *69*, 522–530.
(38) Kellum, J. A.; Song, M.; Li, J. *Crit. Care* **2004**, *8*, 331–336.